



# Hippocampal synaptic failure is an early event in experimental parkinsonism with subtle cognitive deficit

Arantzazu Belloso-Iguerategui,<sup>1</sup> Marta Zamarbide,<sup>1</sup> Leyre Merino-Galan,<sup>1,2,†</sup> Tatiana Rodríguez-Chinchilla,<sup>1</sup> Belén Gago,<sup>3</sup> Enrique Santamaria,<sup>4,5</sup> Joaquín Fernández-Irigoyen,<sup>4,5</sup> Carl W. Cotman,<sup>6</sup> G. Aleph Prieto,<sup>6,7</sup> Ana Quiroga-Varela,<sup>1,5,†,§</sup> and María Cruz Rodríguez-Oroz<sup>1,5,8§</sup>

<sup>§</sup>These authors contributed equally to this work.

Learning and memory mainly rely on correct synaptic function in the hippocampus and other brain regions. In Parkinson's disease, subtle cognitive deficits may even precede motor signs early in the disease. Hence, we set out to unravel the earliest hippocampal synaptic alterations associated with human  $\alpha$ -synuclein overexpression prior to and soon after the appearance of cognitive deficits in a parkinsonism model.

We bilaterally injected adeno-associated viral vectors encoding A53T-mutated human  $\alpha$ -synuclein into the substantia nigra of rats, and evaluated them 1, 2, 4 and 16 weeks post-inoculation by immunohistochemistry and immunofluorescence to study degeneration and distribution of  $\alpha$ -synuclein in the midbrain and hippocampus. The object location test was used to evaluate hippocampal-dependent memory. Sequential window acquisition of all theoretical mass spectrometry-based proteomics and fluorescence analysis of single-synapse long-term potentiation were used to study alterations to protein composition and plasticity in isolated hippocampal synapses. The effect of L-DOPA and pramipexole on long-term potentiation was also tested.

Human  $\alpha$ -synuclein was found within dopaminergic and glutamatergic neurons of the ventral tegmental area, and in dopaminergic, glutamatergic and GABAergic axon terminals in the hippocampus from 1 week post-inoculation, concomitant with mild dopaminergic degeneration in the ventral tegmental area. In the hippocampus, differential expression of proteins involved in synaptic vesicle cycling, neurotransmitter release and receptor trafficking, together with impaired long-term potentiation were the first events observed (1 week post-inoculation), preceding cognitive deficits (4 weeks post-inoculation). Later on, at 16 weeks post-inoculation, there was a deregulation of proteins involved in synaptic function, particularly those involved in the regulation of membrane potential, ion balance and receptor signalling. Hippocampal long-term potentiation was impaired before and soon after the onset of cognitive deficits, at 1 and 4 weeks post-inoculation, respectively. L-DOPA recovered hippocampal long-term potentiation more efficiently at 4 weeks post-inoculation than pramipexole, which partially rescued it at both time points.

Overall, we found impaired synaptic plasticity and proteome dysregulation at hippocampal terminals to be the first events that contribute to the development of cognitive deficits in experimental parkinsonism. Our results not only point to dopaminergic but also to glutamatergic and GABAergic dysfunction, highlighting the relevance of the three neurotransmitter systems in the ventral tegmental area-hippocampus interaction from the earliest stages of parkinsonism. The proteins identified in the current work may constitute potential biomarkers of early synaptic damage in the hippocampus and hence, therapies targeting these could potentially restore early synaptic malfunction and consequently, cognitive deficits in Parkinson's disease.

Received February 20, 2023. Revised May 25, 2023. Accepted June 20, 2023. Advance access publication July 4, 2023

© The Author(s) 2023. Published by Oxford University Press on behalf of the Guarantors of Brain.

This is an Open Access article distributed under the terms of the Creative Commons Attribution-NonCommercial License (<https://creativecommons.org/licenses/by-nc/4.0/>), which permits non-commercial re-use, distribution, and reproduction in any medium, provided the original work is properly cited. For commercial re-use, please contact [journals.permissions@oup.com](mailto:journals.permissions@oup.com)

- 1 Neuroscience Program, Center for Applied Medical Research (CIMA), Universidad de Navarra, 31008 Pamplona, Spain
- 2 Neuroscience Department, University of the Basque Country (UPV/EHU), 48940 Leioa, Spain
- 3 Faculty of Medicine, IBIMA Plataforma BIONAND, Universidad de Málaga, 29016 Málaga, Spain
- 4 Clinical Neuroproteomics Unit, Proteomics Platform, Proteored-ISCI, Navarrabiomed, Complejo Hospitalario de Navarra (CHN), Universidad Pública de Navarra (UPNA), 31008 Pamplona, Spain
- 5 Neurosciences and Mental Health Area, Navarra Institute for Health Research (IdiSNA), 31008 Pamplona, Spain
- 6 Institute for Memory Impairments and Neurological Disorders, University of California-Irvine, Irvine, CA 92697, USA
- 7 Instituto de Neurobiología, Universidad Nacional Autónoma de México, 76010 Querétaro, México
- 8 Neurology Department, Clínica Universidad de Navarra (CUN), 31008 Pamplona, Spain

<sup>†</sup>Present address: Ben Towne Center for Childhood Cancer Research, Seattle Children's Research Institute, Seattle, WA 98101, USA

<sup>‡</sup>Present address: Neurodegeneration and Neuroinflammation Group, Girona Biomedical Research Institute (IDIBGI), 17190 Salt, Spain

Correspondence to: María Cruz Rodríguez-Oroz  
 Clínica Universidad de Navarra  
 Avda. Pio XII 36, 31008 Pamplona, Spain  
 E-mail: mcroroz@unav.es

**Keywords:** Parkinson's disease; synapse; hippocampus;  $\alpha$ -synuclein; cognitive impairment

## Introduction

Parkinson's disease is characterized by the degeneration of dopaminergic neurons in the substantia nigra pars compacta (SNpc), leading to dopamine depletion in the striatum that heralds the motor abnormalities of the disease.<sup>1</sup> Although classically considered a motor disorder, numerous non-motor symptoms are also evident in Parkinson's disease, some of which may even precede the onset of motor manifestations.<sup>2,3</sup> Among these, cognitive decline may arise during the earliest stages of Parkinson's disease, affecting executive functions and working memory, which could progress to dementia in advanced stages of the disease.<sup>4,5</sup>

The presence of intracellular protein aggregates, of which one of the main components is  $\alpha$ -synuclein ( $\alpha$ -syn), is a pathological hallmark of Parkinson's disease.<sup>1</sup> Among the abnormalities associated with cognitive decline in Parkinson's disease, dysfunction of the striato-frontal dopaminergic system in early stages, and the subsequent spreading of  $\alpha$ -syn aggregates to limbic and cortical regions, are particularly relevant.<sup>6</sup> The hippocampus is a structure of the limbic system classically related to learning and memory, as well as to emotion, decision-making and reward-related processes through its connections with other limbic structures.<sup>7–10</sup> Multiple functional and structural imaging studies have linked hippocampal hypometabolism and atrophy with memory impairment and progression into dementia in patients with Parkinson's disease.<sup>11,12</sup> In addition, altered dopaminergic function in the hippocampus is associated with several neuropsychiatric and behavioural disturbances in Parkinson's disease.<sup>13</sup> The mesolimbic dopaminergic pathway from the ventral tegmental area (VTA) innervates the hippocampus, where dopamine facilitates synaptic plasticity and promotes long-term memory storage.<sup>7,14,15</sup> Interestingly, the dopaminergic neurons of the VTA are also affected in Parkinson's disease with a varying degree of neuronal loss (31% to 77%).<sup>16,17</sup> Importantly, the VTA contains not only dopaminergic, but also

populations of GABAergic and glutamatergic neurons that regulate local VTA dopaminergic neuronal activity. These neurons also send long-range connections to limbic regions that include the hippocampus, regulating reward-related, as well as learning and memory processing.<sup>18,19</sup> However, little is known about the relative contribution of these dopaminergic and non-dopaminergic projections from the VTA to the earliest events that lead to hippocampal dysfunction and memory impairment in Parkinson's disease.<sup>20</sup>

Synapses are extremely dynamic structures that are constantly being formed, eliminated and reshaped. Synaptic plasticity involves the activity-dependent remodelling of synaptic transmission and it enables new information to be acquired.<sup>21</sup> Indeed, long-term potentiation (LTP) in the hippocampus is widely recognized as the cellular basis of long-term memory. In molecular terms, hippocampal LTP depends on the activation of NMDA receptors (NMDARs) and the subsequent insertion of AMPA receptors (AMPA) in the postsynaptic membrane, triggering a postsynaptic excitatory response.<sup>22,23</sup> Dopamine is a known modulator of LTP<sup>14,24</sup> and dopaminergic receptors are located in the postsynaptic density (PSD)<sup>25</sup> where they interact directly with NMDARs.<sup>26–28</sup> In the hippocampus, dopamine enhances LTP by activating D1-like receptors (D1Rs and D5Rs),<sup>7,14</sup> thereby increasing AMPAR expression at the cell surface.<sup>29</sup> The role of D2-like receptors (D2Rs, D3Rs and D4Rs) is less well understood and although D2Rs have been proposed to facilitate LTP,<sup>30,31</sup> D3Rs and D4Rs have been shown to both facilitate and inhibit LTP.<sup>32–36</sup>

Synaptic dysfunction is an early neurobiological event in the development of Parkinson's disease due to the accumulation of  $\alpha$ -syn in presynaptic terminals.<sup>37,38</sup> Alterations to proteins involved in synapse organization and neurotransmitter regulation, impaired dopamine release, deficient synaptic vesicle (SV) recycling and deficits in LTP have been described in the striatum,<sup>39–42</sup> and limbic regions like the hippocampus<sup>43–45</sup> and prefrontal

cortex<sup>46</sup> of animal models and patients with advanced Parkinson's disease.

Therefore, our hypothesis is that abnormal  $\alpha$ -syn accumulation in dopaminergic and non-dopaminergic VTA neurons projecting to the hippocampus could negatively affect hippocampal synaptic function, compromising their interactions within the limbic system and ultimately leading to the appearance of memory deficits. Hence, our objectives here were to analyse the distribution of  $\alpha$ -syn overexpressed in the VTA neurons and the axon terminals in the hippocampus as well as to evaluate the biochemical and functional alterations in hippocampal synapses in a model of parkinsonism before and soon after the onset of motor and cognitive deficits. As such, we inoculated the SNpc of rats with adeno-associated viral vectors (AAVs) overexpressing an A53T-mutated  $h\alpha$ -syn, inducing its expression in both the SNpc and VTA. We then studied the distribution of the overexpressed  $h\alpha$ -syn and investigated the potential functional consequences of its expression in the hippocampus.

## Materials and methods

### Animal model

Adult male Sprague-Dawley rats (300 g, Charles River) were housed under standard conditions (70% humidity, 22°C, regular 12 h light/dark cycle) with *ad libitum* access to food and water. All experimental procedures were approved by the ethics committee for animal research at the Biodonostia Health Research Institute (CEEA16/11; ANIMA4-002) and CIMA-Universidad de Navarra (108-17), and they were carried out following the guidelines of the Spanish Government (RD53/2013) and the European Union Council Directive (2010/63/EU). All efforts were made to avoid and/or alleviate animal suffering and to reduce the number of animals used.

AAVs (AAV2/9-CMV-WPRE) inducing the overexpression of either A53T  $h\alpha$ -syn ( $3.9 \times 10^{13}$  genomic particles/ml) or empty vectors (EVV:  $1 \times 10^{12}$  genomic particles/ml) were custom ordered from the University of Bordeaux (France). The two experimental groups (AAV- $h\alpha$ -syn or AAV-EVV) were subdivided according to the final time point post-inoculation (p.i.: 1, 2, 4 and 16 weeks), conducting a cross-sectional study. Rats were anaesthetized with isoflurane in oxygen-enriched air (2%) and placed in a stereotactic head frame (Stoelting). The AAVs were injected bilaterally into two points of the SNpc (1  $\mu$ l per site, 0.2  $\mu$ l/min).<sup>39</sup> The co-ordinates from Bregma used were: (i) anteroposterior -4.9, lateral  $\pm$ 2.2, ventral -7.7 mm; and (ii) anteroposterior -5.4, lateral  $\pm$ 2.0, ventral -7.7 mm.<sup>47</sup>

### Behavioural studies

Motor function was evaluated using the adjusting stepping and the open field tests (OFT), and cognitive performance with the object location test (OLT) ( $n = 8$ /group and time point, 1 and 4 weeks p.i.). In the stepping test, the average number of adjusting steps taken with each forepaw in either direction (adduction and abduction) were analysed.<sup>39</sup> In the OFT, the total distance travelled (cm) and the total velocity (cm/s) were evaluated over a 15 min exploration time.<sup>39</sup> The OLT was performed after the OFT in the same arena and considering the OFT as the habituation phase for the OLT. During the first phase of the OLT, the animals were exposed to two identical objects placed in the far corners for 5 min. In the test phase (5 min later), one of the objects was moved to the opposite corner and the animals were allowed to explore the arena for 5 min (Fig. 1A). The time spent exploring each object during the test phase was measured and a discrimination index was calculated as follows:

$$\text{Discrimination Index} = \frac{\text{time exploring displaced object} - \text{time exploring stationary object}}{\text{total exploring time}} \quad (1)$$

Between different tests and trials, the arena and objects were cleaned with 70% ethanol to minimize any olfactory cues. The OFT and OLT tests were video recorded using a camera mounted above the arena, and an experimenter blind to the group and time point analysed the data using the Ethovision X13 software (Noldus).

### Immunohistochemistry and immunofluorescence

Animals ( $n = 4$ /group and time point: 1, 2, 4 and 16 weeks p.i.) were perfused transcardially with 4% paraformaldehyde in phosphate buffer (pH 7.4), and their brains were removed, post-fixed overnight and then transferred to a cryoprotective solution (pH 7.4). Serial coronal sections (50  $\mu$ m thick) were collected and immunohistochemistry and immunofluorescence were performed on free-floating sections. Immunohistochemistry was performed on sections containing the SNpc/VTA and the hippocampus to evaluate  $h\alpha$ -syn expression, or the SNpc/VTA to evaluate tyrosine hydroxylase (TH) expression. Images were acquired on an Aperio CS2 digital pathology slide scanner (Leica Biosystems), and  $h\alpha$ -syn immunoreactivity and the number of TH<sup>+</sup> cells in the SNpc/VTA were assessed by densitometric analysis and stereology, respectively.<sup>39</sup> Triple immunofluorescence staining was performed on sections

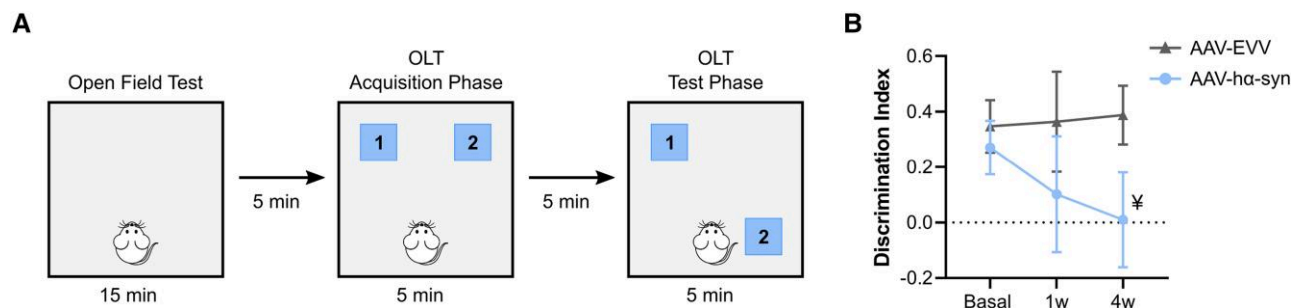


**Figure 1 Cognitive evaluation.** (A) Schematic representation of the object location test (OLT). (B) Discrimination index before surgery (basal) and 1 and 4 weeks (w) post-inoculation (p.i.) in AAV-EVV and AAV- $h\alpha$ -syn animals. The values are represented as the mean  $\pm$  SEM and they were analysed with a two-way ANOVA followed by Bonferroni's *post hoc* test:  $^{\text{¥}}P = 0.084$  versus AAV-EVV. No differences were found compared to the basal state in either the AAV-EVV and AAV- $h\alpha$ -syn groups ( $n = 8$  for each group and time point). AAV = adeno-associated viral vector; EEV = empty vector;  $h\alpha$ -syn = human  $\alpha$ -synuclein.

containing the VTA to confirm the presence of  $\alpha$ -syn in dopaminergic (TH<sup>+</sup>) and glutamatergic (vGlut2<sup>+</sup>) neurons, and double immunofluorescent staining was performed on sections containing the hippocampus to elucidate the dopaminergic (TH<sup>+</sup>), glutamatergic (vGlut2<sup>+</sup>) or GABAergic (GABA<sup>+</sup>) nature of  $\alpha$ -syn<sup>+</sup> fibres. Images were acquired on a Zeiss LSM 800 confocal laser microscope (Carl Zeiss). See [Supplementary material](#) for further details.

### Quantitative proteomics by SWATH-MS and bioinformatics analysis

Animals ( $n = 5$ /group and time point: 1, 2, 4 and 16 weeks p.i.) were anaesthetized deeply and sacrificed, their brains were removed quickly, and the hippocampus was extracted and immediately frozen on dry ice for storage at  $-80^{\circ}\text{C}$ . The synaptosomal fraction was isolated from the hippocampal tissue and the samples were subjected to sequential window acquisition of all theoretical mass spectra-mass spectrometry (SWATH-MS), as described previously by our group.<sup>39</sup> Significantly dysregulated regulatory/metabolic pathways were identified using Metascape.<sup>48</sup> The human and rat  $\alpha$ -syn interactome was obtained from the curated Biological General Repository for Interaction Datasets (BioGRID: <https://thebiogrid.org>).<sup>49</sup> The synaptic ontology analysis was performed using the SynGo platform (<https://syngoportal.org>).<sup>50</sup> See [Supplementary material](#) for details.

### Fluorescence analysis of single-synapse LTP

After the behavioural studies, the animals ( $n = 8$ /group and time point: 1 and 4 weeks p.i.) were anaesthetized and sacrificed. Their brains were quickly removed, the hippocampus was extracted, and the synaptosome-enriched P2 fraction was isolated. Synaptosomes were subjected to chemical stimulation of LTP (cLTP), fluorescent labelling of postsynaptic GluA1 and presynaptic neuroligin-1 ( $\text{Nrx1}\beta$ ), and analysis by flow cytometry, as described previously.<sup>51</sup> Cell membrane integrity was assessed through Calcein AM staining (100 nM: Thermo Fisher Scientific, Cat. No. 65-0853-78). Additionally, the effect of the dopamine precursor L-DOPA (30  $\mu\text{M}$ : Sigma-Aldrich, Cat. No. D1507) and the dopaminergic agonist pramipexole (PPX, 10  $\mu\text{M}$ : Sigma-Aldrich, Cat. No. D1237) on synaptic functionality was assessed. Samples were acquired using a FACSCanto II System (BD Biosciences) and they were analysed with FlowJo v10 software (FlowJo LLC). See [Supplementary material](#) for more details.

### High-performance liquid chromatography

The concentration of glutamate and GABA in the hippocampus was determined by high-performance liquid chromatography (HPLC) with electrochemical detection (DECADE: Antec Scientific) and with a high-sensitivity analytic flow cell (VT-03). The electrode was set at 0.7 V and the column used (Biophase ODS 5 mm,  $4.6 \times 150$  mm) incorporated precolumn derivatization. The results were expressed as ng/mg of wet tissue.

### Statistical analysis

Statistical analyses were performed using GraphPad Prism 8.0 software (GraphPad Software Inc.). The normality of the data distribution was assessed using the Kolmogorov-Smirnov test and variance equality with Levene's test. Non-parametric tests were used when the data did not meet the assumptions of the parametric tests. An unpaired t-test or Mann-Whitney test was performed when comparing two

independent groups. One-way ANOVA, two-way ANOVA, or a Kruskal Wallis test, with either Tukey's, Dunn's or Bonferroni's post hoc tests, were performed when comparing multiple groups. The group data are represented as the mean  $\pm$  standard error of the mean (SEM) and statistically significant differences were set at  $P < 0.05$ .

## Results

### Motor dysfunction arises at 4 weeks post-inoculation along with mild hippocampal-dependent cognitive deficits

In the OLT, which specifically assesses hippocampal-dependent spatial memory, the AAV- $\alpha$ -syn animals had a tendency towards impaired spatial memory at 4 weeks p.i. relative to the AAV-EVV animals ( $P = 0.084$ ) (Fig. 1B). Although in the AAV- $\alpha$ -syn animals there was a progressive mild decline in spatial memory, that was not observed in the AAV-EVV rats, this result was not statistically significant (Fig. 1B). Moreover, the AAV- $\alpha$ -syn animals had mild motor impairment at 4 weeks p.i., taking fewer adjusted steps ( $P < 0.01$ ), and traveling less distance and slower in the OFT ( $P < 0.05$ ) (Supplementary Fig. 1A and B). Thus, this animal model appears to be well suited to study the molecular alterations in the prodromal stage (1 week p.i.) and at the onset of behavioural deficits at 4 weeks p.i.

### Human $\alpha$ -synuclein spreads from nigral to ventral tegmental area neurons causing dopaminergic loss

Human  $\alpha$ -syn overexpression was observed bilaterally in the SNpc and the adjacent VTA from as early as 1 week p.i., and it had accumulated significantly at 4 and 16 weeks p.i. ( $P < 0.05$  versus 1 week p.i.) (Fig. 2A and Supplementary Fig. 1C). In the VTA,  $\alpha$ -syn was observed within dopaminergic (TH<sup>+</sup>) and glutamatergic (vGlut2<sup>+</sup>) neuronal somas and fibres (Fig. 2B). Owing to the technical difficulties in staining GABAergic neurons, it was not possible to confirm or exclude the presence of  $\alpha$ -syn in these neurons. A mild bilateral loss of TH<sup>+</sup> cells was observed in the VTA from 1 week p.i. (42% cell loss versus AAV-EVV,  $P < 0.05$ ) (Fig. 2C) and as described previously,<sup>39,53</sup> there was significant bilateral TH<sup>+</sup> cell loss in the SNpc of AAV- $\alpha$ -syn animals from 4 weeks p.i. onwards (31% versus AAV-EVV,  $P < 0.05$ ) (Supplementary Fig. 1D).

### Human $\alpha$ -synuclein is expressed early in the hippocampus at dopaminergic and non-dopaminergic axon terminals

We observed a progressive accumulation of  $\alpha$ -syn in the hippocampus from 1 week p.i. (Fig. 2D), and this was enhanced significantly at 4 and 16 weeks p.i. within all the hippocampal subfields ( $P < 0.05$  versus 1 week p.i.; Fig. 2D and E). In the dentate gyrus (DG),  $\alpha$ -syn expression was observed in the hilus from 1 week p.i. and in the granular cell layer from 2 weeks p.i. In the CA1 subfield, we observed  $\alpha$ -syn accumulation in the stratum oriens, pyramidal cell layer and stratum radiatum as early as 1 week p.i., whereas in the stratum lacunosum-moleculare (LMol) immunostaining became more prominent at 16 weeks p.i. In the CA3 region,  $\alpha$ -syn was mainly observed in the stratum lucidum at 4 weeks p.i., expanding through the different layers at 16 weeks p.i.

We next carried out a qualitative assessment of the localization of  $\alpha$ -syn within dopaminergic (TH<sup>+</sup>), glutamatergic (vGlut2<sup>+</sup>) and GABAergic (GABA<sup>+</sup>) projections to the hippocampus.  $\alpha$ -syn accumulated in dopaminergic and non-dopaminergic fibres from the earliest

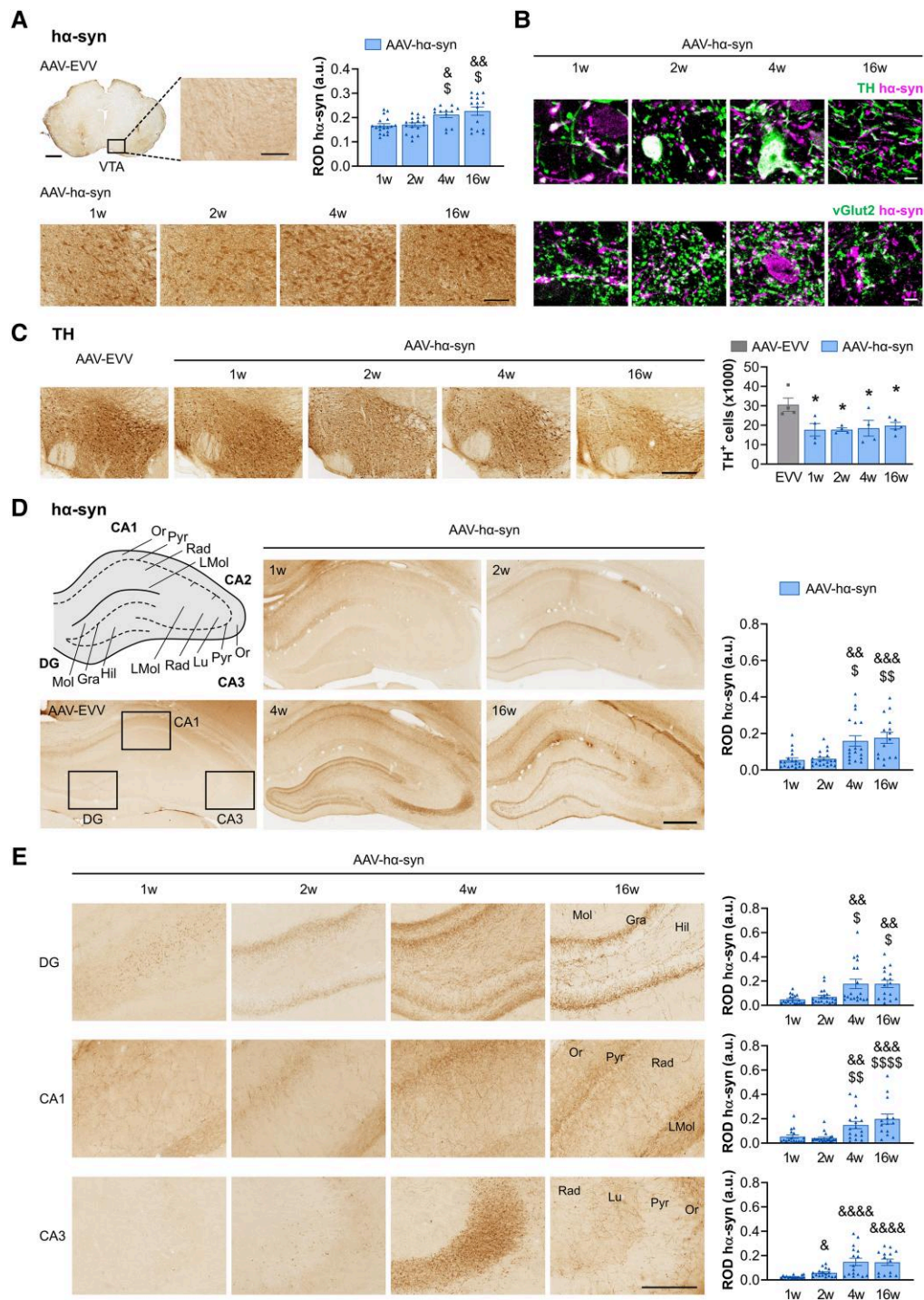


**Figure 2** Histological characterization of the VTA and hippocampus. (A) Representative photomicrographs of human  $\alpha$ -synuclein (ha-syn) staining in the ventral tegmental area (VTA) in AAV-EVV and AAV-ha-syn rats at 1, 2, 4 and 16 weeks (w) post-inoculation (p.i.). Scale bars: low magnification photomicrographs = 1 mm and high magnification photomicrographs = 100  $\mu$ m. Relative optical density (ROD) quantification of ha-syn expression. (B) Representative high magnification photomicrographs of ha-syn co-localization with tyrosine hydroxylase (TH) and vGlut2 staining in the VTA. Scale bars = 5  $\mu$ m. (C) Representative photomicrographs of TH staining in the VTA of AAV-EVV and AAV-ha-syn animals at 1, 2, 4 and 16 weeks p.i. Scale bar = 300  $\mu$ m. Bilateral quantification of TH<sup>+</sup> neurons. (D) Schematic representation of the anatomical regions of the hippocampus. Representative photomicrographs of ha-syn staining in AAV-EVV and AAV-ha-syn animals at 1, 2, 4 and 16 weeks p.i. Scale bar = 500  $\mu$ m. ROD analysis of ha-syn expression in the whole hippocampus. (E) Representative higher magnification photomicrographs of ha-syn staining in the DG, CA1 and CA3 regions of the hippocampus in the AAV-ha-syn animals at 1, 2, 4 and 16 weeks p.i. Scale bar = 200  $\mu$ m. ROD analysis of ha-syn expression in DG, CA1 and CA3 regions. The different anatomical regions and layers of the hippocampus are indicated as follows: dentate gyrus (DG)—molecular layer (Mol), granular cell layer (Gra), and hilus (Hil); CA1—stratum oriens (Or), pyramidal cell layer (Pyr), stratum radiatum (Rad) and stratum lacunosum-moleculare (LMol); CA3—Or, Pyr, stratum lucidum (Lu) and LMol. All values are presented as the mean  $\pm$  SEM and they were analysed using a Kruskal-Wallis test followed by Dunn's post hoc test:  $^{\&}P < 0.05$ ,  $^{\&\&}P < 0.01$ ,  $^{\&\&\&}P < 0.001$ ,  $^{\&\&\&\&}P < 0.0001$  versus 1 week p.i.;  $^{\$}P < 0.05$ ,  $^{\$\$}P < 0.01$ ,  $^{\$\$\$\$}P < 0.0001$  versus 2 weeks p.i.;  $^{\#}P < 0.05$  versus AAV-EVV ( $n = 4$  for each group and time point). AAV = adeno-associated viral vector; EVV = empty vector.

time points (1 and 2 weeks p.i.) (Fig. 3A). Specifically,  $\alpha$ -syn was detected within all three types of projections in the hilus of the DG and CA1 region from 1 week p.i., in glutamatergic and GABAergic fibres of the granule cell layer in the DG from 2 weeks p.i., in dopaminergic and glutamatergic fibres in the LMol of the CA1 region at 16 weeks p.i., and exclusively within glutamatergic fibres in the CA3 region from 4 weeks p.i. (Fig. 3A, summarized in Fig. 3B).

### Proteostatic alterations in hippocampal synapses are present from the onset of human $\alpha$ -synuclein expression at 1 week post-inoculation

A total of 7958 individual proteins were identified by SWATH-MS proteomics in hippocampal synaptosomes, of which 131 proteins were significantly deregulated following AAV- $\alpha$ -syn inoculation when all time points were considered (1, 2, 4 and 16 weeks p.i.) (Fig. 4A and B and Supplementary Table 1). Only a few proteins overlapped between the different time points (Fig. 4B).

The earliest changes occurred at 1 week p.i., when 50 differentially expressed proteins (DEPs) were found (Fig. 4A and B). Some of these proteins were associated with transport along microtubules, cytosolic transport, regulation of protein binding and ATP biosynthesis (Fig. 4D). At 2 weeks p.i., 34 DEPs were detected (Fig. 4A and B), mainly linked to actin filament-based movement and processes, protein localization to the membrane, the regulation of intracellular transport or of adenosine diphosphate-ribosylation factor (ARF) protein signalling, signal release, postsynaptic organization or lysosomal transport (Fig. 4D). At 4 weeks p.i., there were 16 DEPs identified (Fig. 4A and B), although the ontology analysis did not reveal any enrichment of a particular biological pathway. Finally, at 16 weeks p.i., there were 28 DEPs (Fig. 4A and B), some of which were related to the regulation of postsynaptic membrane potential, cation homeostasis, cell surface receptor signalling, G protein-coupled receptor (GPCR)/Gi signalling or tRNA metabolism (Fig. 4D).

Based on a clustering analysis of the DEPs, only two proteins overlapped with the rat  $\alpha$ -syn interactome and 12 proteins with the human interactome (Fig. 4C). Of note, most of these  $\alpha$ -syn interactors were altered by 1 week p.i. (MAP2K1, APP, CNP, INA, BCAS1, FBOX2, SNCB and MAP2), and they are involved in the assembly of the synapses, and in the regulation of synaptic transmission, the presynaptic SVs and postsynaptic receptor trafficking (Supplementary Table 2).

When all the DEPs were considered, 24 proteins were mapped to SynGO annotated genes. This in-depth synaptic gene ontology analysis revealed that changes in structural proteins occurred at the presynaptic and postsynaptic levels from 1 week p.i., particularly affecting the cytoskeleton and functionally active domains (the presynaptic active zone and the PSD) (Supplementary Fig. 2 and Supplementary Table 3). DEPs were also involved in functional biological processes like synapse organization, chemical synaptic transmission, or SV trafficking, processes that are crucial for neurotransmitter release. In addition, several of these proteins were involved in the regulation of the membrane potential at 16 weeks p.i. (Supplementary Fig. 2 and Supplementary Table 2).

### Impaired hippocampal long-term potentiation precedes cognitive deficits and is partially rescued by dopaminergic treatments

We evaluated LTP directly at synapses using fluorescence analysis of single-synapse (FASS)-LTP, a method that enables cLTP to be studied in isolated synaptosomes following NMDAR activation by depolarization in the presence of the NMDAR co-agonist glycine

(as first described by Prieto and coworkers,<sup>51,54</sup> and replicated by others<sup>55</sup>). FASS-LTP identifies potentiated synaptosomes by flow cytometry after surface labelling with antibodies specific to extracellular epitopes of the GluA1 AMPAR subunit and Nr1 $\beta$ , a pre-synaptic adhesion molecule stabilized at the membrane surface by synaptic activity. GluA1 (postsynaptic) and Nr1 $\beta$  (presynaptic) double labelling ensures that intact synaptosomes that contain both pre- and post-synaptic elements are analysed.

We evaluated cLTP at the onset of  $\alpha$ -syn expression in the SNpc/VTA and hippocampus (1 week p.i.), as well as at the onset of a tendency towards cognitive decline (4 weeks p.i.). In size-gated synaptosomes, we first evaluated cell membrane integrity with Calcein AM and found no differences between the different experimental groups (Fig. 5A and Supplementary Fig. 3E and F). We next analysed GluA1<sup>+</sup>/Nr1 $\beta$ <sup>+</sup> events within Calcein<sup>+</sup> synaptosomes (Fig. 5A) and as expected, there was an increase in GluA1<sup>+</sup>/Nr1 $\beta$ <sup>+</sup> double-labelled synaptosomes after cLTP stimulation in the AAV-EVV animals relative to the unstimulated basal state (% cLTP = 175.3  $\pm$  65.2 at 1 week p.i. and % cLTP = 187.0  $\pm$  108.8 at 4 weeks p.i.). Notably, there was a decrease in cLTP in the AAV- $\alpha$ -syn animals compared to the AAV-EVV animals at 1 week (% cLTP = 87.7  $\pm$  23.1;  $P < 0.01$ ) and 4 weeks p.i. (% cLTP = 75.0  $\pm$  42.3;  $P < 0.01$ ) (Fig. 5B).

Dopaminergic drugs influence hippocampal LTP by acting on the dopaminergic receptors located in the PSD.<sup>14</sup> Using FASS-LTP, we evaluated the effect of two dopaminergic treatments (PPX and *l*-DOPA). Exposing synaptosomes from AAV- $\alpha$ -syn animals to PPX partially rescued cLTP at both time points relative to the vehicle (% cLTP = 120.0  $\pm$  30.5 at 1 week p.i. and % cLTP = 117.4  $\pm$  70.5 at 4 weeks p.i.;  $P < 0.05$ ) (Fig. 5B), whereas *l*-DOPA fully rescued cLTP in the synaptosomes from AAV- $\alpha$ -syn animals relative to the vehicle at 4 weeks p.i. (% cLTP = 190.6  $\pm$  87.3;  $P < 0.05$ ), but not at 1 week p.i. when the cLTP was still diminished compared to AAV-EVV (% cLTP = 111.0  $\pm$  29.9;  $P < 0.05$ ) (Fig. 5B). Notably, recovery of cLTP in the AAV- $\alpha$ -syn group was significantly greater at 4 weeks p.i. with *l*-DOPA than with PPX ( $P < 0.05$ ) (Fig. 5B). On the other hand, PPX but not *l*-DOPA provoked a decrease in cLTP in the AAV-EVV group at both time points relative to vehicle (PPX: % cLTP = 131.1  $\pm$  50.7 at 1 week p.i. and % cLTP = 121.3  $\pm$  53.7 at 4 weeks p.i.;  $P < 0.05$  versus vehicle; *l*-DOPA: % cLTP = 164.2  $\pm$  74.4 at 1 week p.i. and % cLTP = 147.6  $\pm$  73.54 at 4 weeks p.i.) (Fig. 5B).

A detailed analysis revealed that in the basal (unstimulated) state, there was an increase in GluA1<sup>+</sup>/Nr1 $\beta$ <sup>+</sup> synaptosomes in the AAV- $\alpha$ -syn animals relative to their corresponding AAV-EVV controls at both time points (1 week p.i.: AAV-EVV GluA1<sup>+</sup>/Nr1 $\beta$ <sup>+</sup> = 1.00  $\pm$  0.49 and AAV- $\alpha$ -syn GluA1<sup>+</sup>/Nr1 $\beta$ <sup>+</sup> = 1.94  $\pm$  0.43,  $P < 0.01$  versus AAV-EVV; 4 weeks p.i.: AAV-EVV GluA1<sup>+</sup>/Nr1 $\beta$ <sup>+</sup> = 1.00  $\pm$  0.48 and AAV- $\alpha$ -syn GluA1<sup>+</sup>/Nr1 $\beta$ <sup>+</sup> = 2.90  $\pm$  2.22,  $P < 0.001$  versus AAV-EVV) (Fig. 5C). At 4 weeks p.i., fewer GluA1<sup>+</sup>/Nr1 $\beta$ <sup>+</sup> synaptosomes were observed after cLTP stimulation than in the basal state in the AAV- $\alpha$ -syn group (1 week p.i.: GluA1<sup>+</sup>/Nr1 $\beta$ <sup>+</sup> = 1.67  $\pm$  0.47 and 4 weeks p.i.: GluA1<sup>+</sup>/Nr1 $\beta$ <sup>+</sup> = 1.45  $\pm$  0.77;  $P < 0.01$  versus basal) (Fig. 5C). By contrast, there was a significant increase in the GluA1<sup>+</sup>/Nr1 $\beta$ <sup>+</sup> synaptosomes in the AAV-EVV group after cLTP stimulation relative to the basal state at both time points (1 week p.i.: GluA1<sup>+</sup>/Nr1 $\beta$ <sup>+</sup> = 1.59  $\pm$  0.66,  $P < 0.001$  versus basal; 4 weeks p.i.: GluA1<sup>+</sup>/Nr1 $\beta$ <sup>+</sup> = 1.78  $\pm$  0.92;  $P = 0.0616$  versus basal) (Fig. 5C), indicative of cLTP.

In the AAV-EVV group, incubation with PPX increased the basal levels of GluA1<sup>+</sup>/Nr1 $\beta$ <sup>+</sup> synaptosomes at both time points compared to the vehicle (1 week p.i.: GluA1<sup>+</sup>/Nr1 $\beta$ <sup>+</sup> = 1.31  $\pm$  0.33,  $P < 0.05$  versus vehicle; 4 weeks p.i.: GluA1<sup>+</sup>/Nr1 $\beta$ <sup>+</sup> = 1.87  $\pm$  1.22,  $P < 0.05$  versus vehicle) (Fig. 5C). Despite the basal increase, after cLTP stimulation

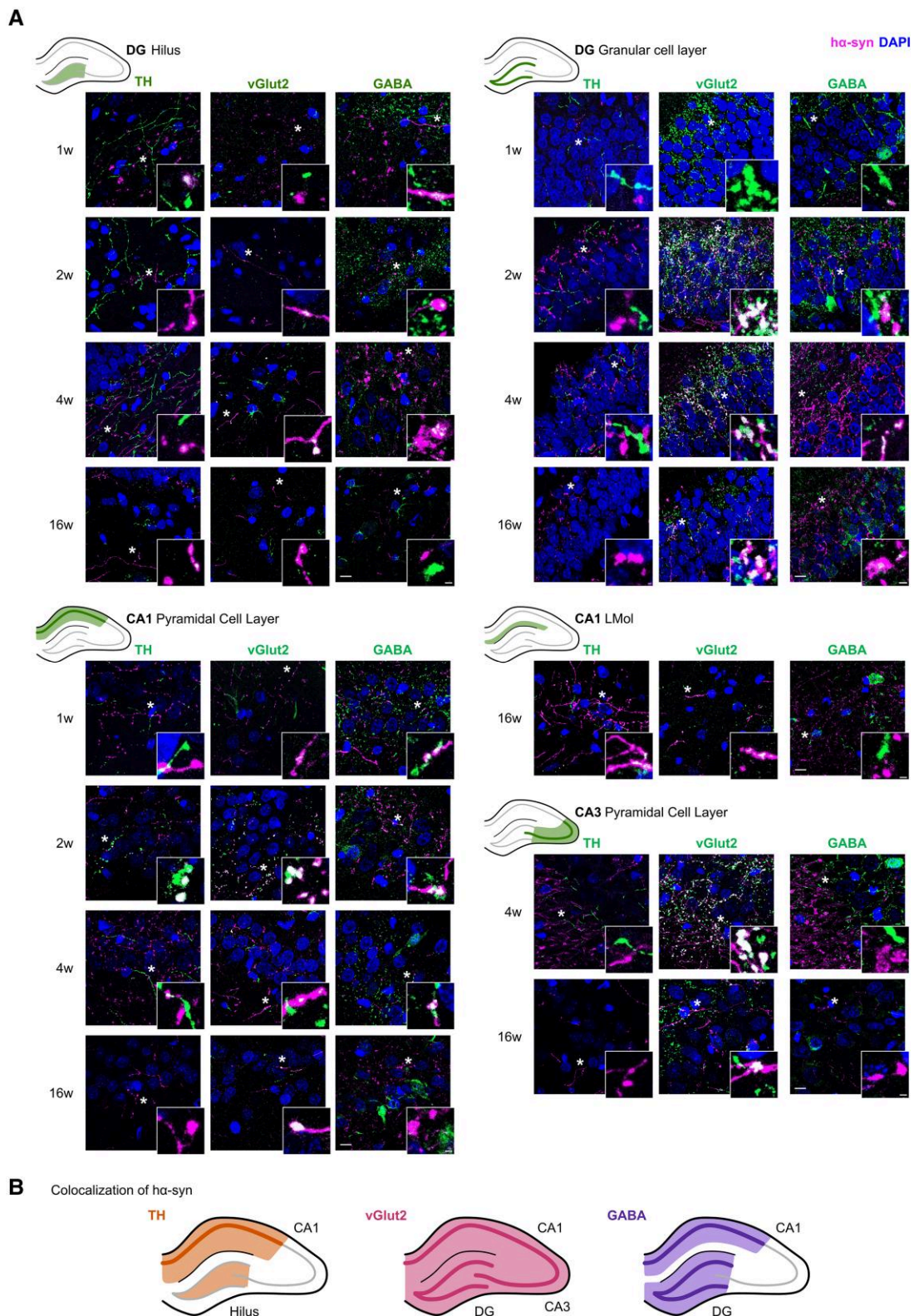


**Figure 3** Expression of  $\alpha$ -syn in dopaminergic ( $TH^+$ ), glutamatergic ( $vGlut2^+$ ) and GABAergic ( $GABA^+$ ) axon terminals in the hippocampus. (A) Representative double immunofluorescence photomicrographs for human  $\alpha$ -synuclein ( $\alpha$ -syn) and tyrosine hydroxylase ( $TH$ ),  $vGlut2$  or  $GABA$  in the hilus and granular cell layer of the dentate gyrus (DG), pyramidal cell layer and stratum lacunosum-moleculare (LMol) of the CA1 region, or pyramidal cell layer of the CA3 region. Scale bar = 10  $\mu m$ . Higher magnification photomicrographs of areas indicated by an asterisk are detailed in the bottom right corner of each photo. Scale bar = 5  $\mu m$  ( $n = 4$  for each group and time point). (B) Schematic representation of the co-localization of  $\alpha$ -syn with  $TH$ ,  $vGlut2$  or  $GABA$  in the distinct hippocampal areas. W = weeks.

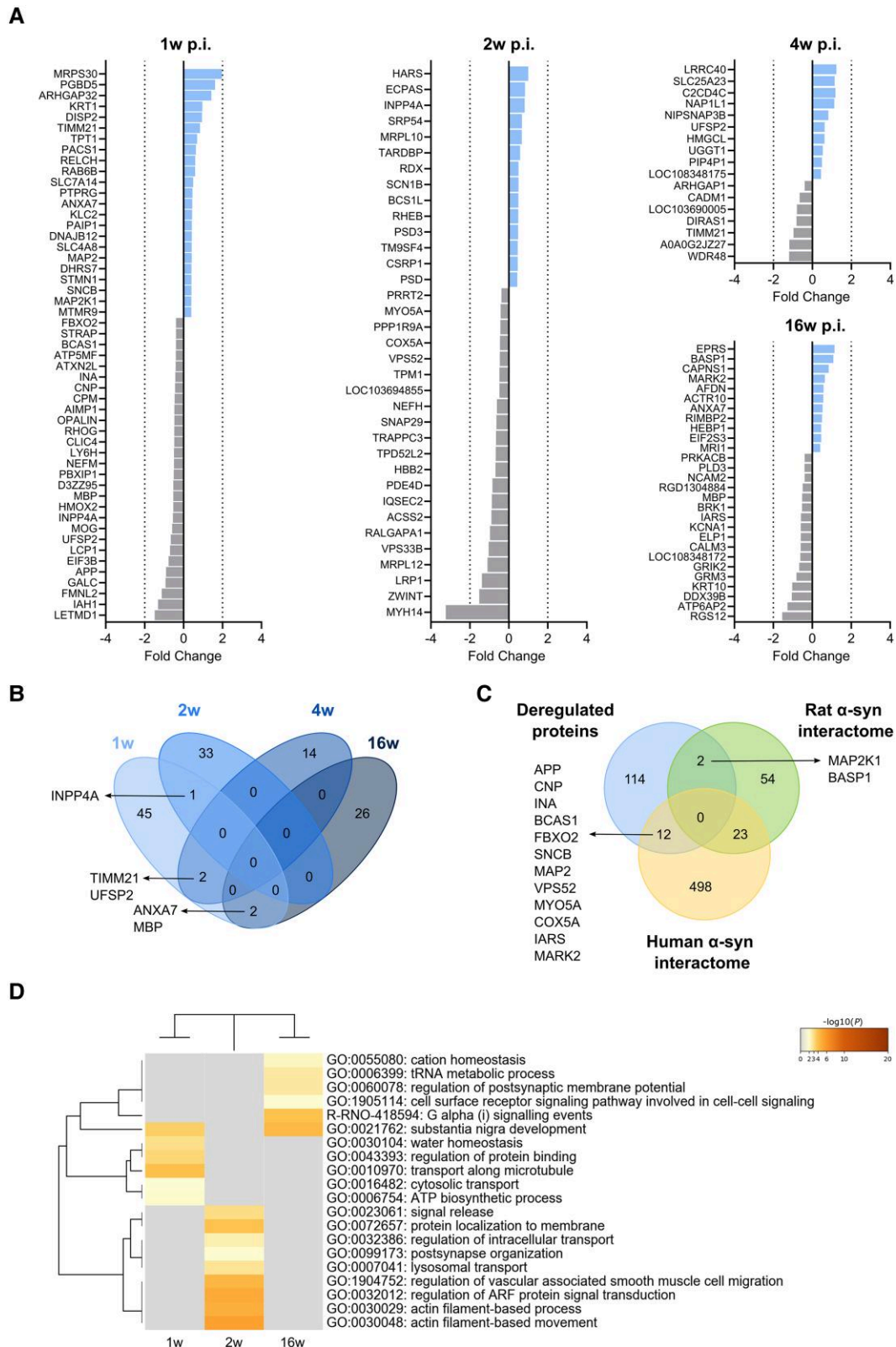


**Figure 4** Deregulated proteins in hippocampal synaptosomes. (A) Differentially expressed proteins (DEPs) at 1, 2, 4 and 16 weeks (w) post-inoculation (p.i.) in the AAV- $\alpha$ -syn animals compared to the AAV-EV group. The colours indicate the fold change of the downregulated (grey) and upregulated proteins (blue). (B) Cluster overlap of DEPs at different time points p.i. (C) Cluster overlap between the overall deregulated proteins and the  $\alpha$ -syn interactome of both rat and human. (D) Heat map showing the enriched biological pathways and gene ontology clusters at 1, 2 and 16 weeks p.i. No enriched pathways were observed at 4 weeks p.i. The colour scale represents the statistical significance and the grey colour indicates a lack of significance ( $n = 5$  for each group and time point). AAV = adeno-associated viral vector; EEV = empty vector;  $\alpha$ -syn = human  $\alpha$ -synuclein.



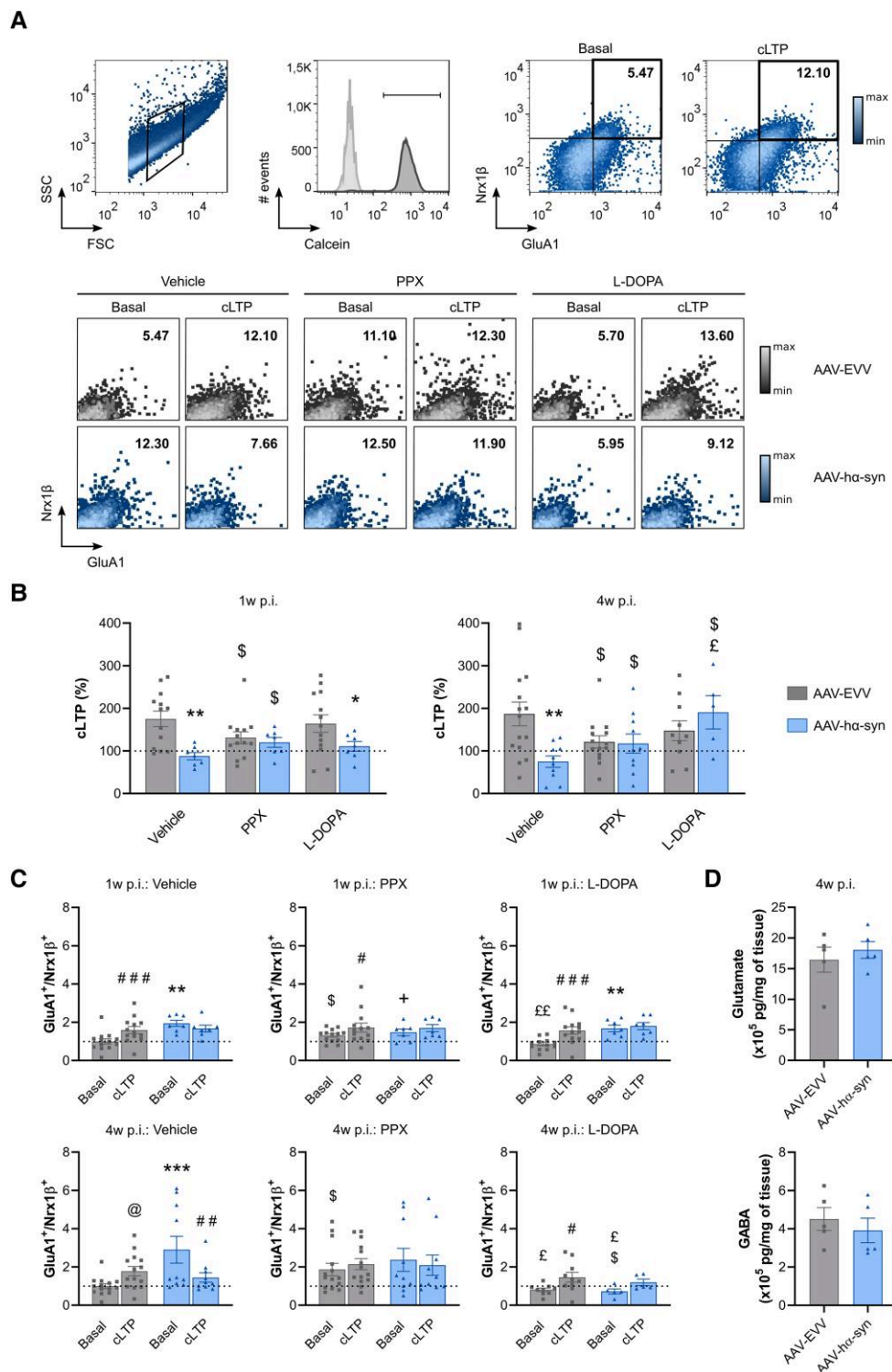


**Figure 5** Flow cytometry evaluation of hippocampal cLTP. (A) Top: Selection of the synaptosomal fraction based on size (FSC) and complexity (SSC). Synaptosomal membrane integrity was evaluated by Calcein AM staining, and GluA1/Nrx1β staining was analysed within Calcein<sup>+</sup> events in the basal state and after chemical long-term potentiation (cLTP) stimulation. Bottom: Representative GluA1<sup>+</sup>/Nrx1β<sup>+</sup> double-positive events at the basal state and after cLTP stimulation in the presence of the vehicle (distilled water), pramipexole (PPX) or L-DOPA. (B) The cLTP (%) at hippocampal synaptosomes in the presence of the vehicle (distilled water), PPX or L-DOPA at 1 and 4 weeks (w) post-inoculation (p.i.). (C) GluA1<sup>+</sup>/Nrx1β<sup>+</sup> double-positive values at the basal state and after cLTP stimulation in the presence of the vehicle (distilled water), PPX and L-DOPA at 1 and 4 weeks p.i. GluA1<sup>+</sup>/Nrx1β<sup>+</sup> values were normalized to the AAV-EVV vehicle condition for each time point, and all the values are represented as the mean ± SEM, and assessed using two-way ANOVA followed by a Tukey's or Bonferroni's post hoc test: #P < 0.05, ##P < 0.01, ###P < 0.001 versus basal; @P = 0.0616 versus basal; \*P < 0.05, \*\*P < 0.01, \*\*\*P < 0.001 versus AAV-EVV; \$P < 0.05 versus vehicle; +P = 0.0639 versus vehicle; <sup>f</sup>P < 0.05, <sup>ff</sup>P < 0.01 versus PPX (n = 8 for each group and time point). (D) Total glutamate and GABA content in the hippocampus at 4 weeks p.i. (n = 5 for each group). The values are represented as the mean ± SEM and assessed with a Mann-Whitney U-test: no significant differences. AAV = adeno-associated viral vector; EVV = empty vector; ha-syn = human α-synuclein.

there was an increase in GluA1<sup>+</sup>/Nrx1β<sup>+</sup> synaptosomes compared to the basal state at 1 week p.i. (GluA1<sup>+</sup>/Nrx1β<sup>+</sup> = 1.72 ± 0.84, *P* < 0.05 versus basal) and at 4 weeks p.i. (GluA1<sup>+</sup>/Nrx1β<sup>+</sup> = 2.15 ± 1.09) (Fig. 5C). L-DOPA had no effect on AAV-EV animals, which showed similar basal GluA1<sup>+</sup>/Nrx1β<sup>+</sup> levels to the vehicle (1 week p.i.: GluA1<sup>+</sup>/Nrx1β<sup>+</sup> = 0.86 ± 0.31; 4 weeks p.i.: GluA1<sup>+</sup>/Nrx1β<sup>+</sup> = 0.81 ± 0.27) and increased levels of GluA1<sup>+</sup>/Nrx1β<sup>+</sup> in cLTP-stimulated synaptosomes compared to the basal state (1 week p.i.: GluA1<sup>+</sup>/Nrx1β<sup>+</sup> = 1.57 ± 0.68, *P* < 0.001 versus basal; 4 weeks p.i.: GluA1<sup>+</sup>/Nrx1β<sup>+</sup> = 1.46 ± 0.80; *P* < 0.05 versus basal) (Fig. 5C).

In the AAV-*hα*-syn animals, PPX partially reduced the basal GluA1<sup>+</sup>/Nrx1β<sup>+</sup> levels at 1 week p.i. compared to the vehicle (1 week p.i.: GluA1<sup>+</sup>/Nrx1β<sup>+</sup> = 1.47 ± 0.45, *P* = 0.0639 versus vehicle; 4 weeks p.i.: GluA1<sup>+</sup>/Nrx1β<sup>+</sup> = 2.37 ± 1.90), but without rescuing cLTP (1 week p.i.: GluA1<sup>+</sup>/Nrx1β<sup>+</sup> = 1.70 ± 0.48; 4 weeks p.i.: GluA1<sup>+</sup>/Nrx1β<sup>+</sup> = 2.09 ± 1.68) (Fig. 5C). Incubation with L-DOPA produced similar results to the vehicle in the AAV-*hα*-syn rats at 1 week p.i. (basal GluA1<sup>+</sup>/Nrx1β<sup>+</sup> = 1.68 ± 0.45, *P* < 0.01 versus AAV-EVV; cLTP GluA1<sup>+</sup>/Nrx1β<sup>+</sup> = 1.80 ± 0.49), while it significantly rescued the basal GluA1<sup>+</sup>/Nrx1β<sup>+</sup> levels at 4 weeks p.i. (basal GluA1<sup>+</sup>/Nrx1β<sup>+</sup> = 0.72 ± 0.30, *P* < 0.05 versus vehicle; cLTP GluA1<sup>+</sup>/Nrx1β<sup>+</sup> = 1.19 ± 0.38) (Fig. 5C). A comparison between the two dopaminergic drugs showed that synaptosomes incubated with L-DOPA had lower basal levels of GluA1<sup>+</sup>/Nrx1β<sup>+</sup> than those exposed to PPX in the AAV-EVV rats (*P* < 0.01 and *P* < 0.05 versus PPX at 1 and 4 weeks p.i., respectively), and in the AAV-*hα*-syn rats at 4 weeks p.i. (*P* < 0.05 versus PPX) (Fig. 5C).

The functional synaptic alterations observed were not accompanied by any change in the total glutamate and GABA content in the hippocampus at 4 weeks p.i. (glutamate × 10<sup>5</sup> pg/mg of tissue: AAV-EVV 16.45 ± 4.60 and AAV-*hα*-syn 18.04 ± 3.06; GABA × 10<sup>5</sup> pg/mg of tissue: AAV-EVV 4.51 ± 1.33 and AAV-*hα*-syn 3.91 ± 1.43) (Fig. 5D). The dopamine levels in the hippocampus were below the threshold for detection by HPLC.

## Discussion

We studied here the early synaptic abnormalities in the hippocampus induced by *hα*-syn overexpression in a model of parkinsonism and its influence on cognitive performance. We show that after the inoculation in the SNpc of AAVs driving *hα*-syn overexpression, *hα*-syn accumulates in the SNpc and VTA, regions where dopaminergic loss reaches 42%. To date, only a few studies have analysed dopaminergic neuronal loss in the VTA of patients with Parkinson's disease at advanced stages,<sup>16,17</sup> and only one has shown a correlation between the loss of dopaminergic VTA neurons and cognitive impairment.<sup>56</sup> However, no studies have as yet been undertaken at the earliest stages of the disease. In the MPTP monkey model, there is a loss of dopaminergic neurons of the SNpc but also the VTA prior to the appearance of parkinsonian motor signs.<sup>57</sup> The data obtained here suggest that this VTA degeneration may be an early event leading to dopaminergic mesocorticolimbic pathway dysfunction and the onset of cognitive decline.

In these studies, both dopaminergic TH<sup>+</sup> and glutamatergic vGluT2<sup>+</sup> VTA neurons overexpress *hα*-syn. Both glutamatergic and GABAergic neurons of the VTA are known to project to the hippocampus and they are involved in memory encoding, as well as goal- and reward-directed behaviours.<sup>19</sup> We assessed the distribution of *hα*-syn in the hippocampus by immunofluorescence and we found that *hα*-syn spreads early into the hippocampus, mainly in the hilus and granular cell layer of the DG but also, in the CA1 region, from as early as 1 week p.i., areas involved in initial memory

encoding and consolidation, and in retrieval, respectively.<sup>58</sup> Furthermore, *hα*-syn was present in dopaminergic, glutamatergic and GABAergic axon terminals, coinciding with the known projections from the VTA to the hippocampus,<sup>18,59–61</sup> yet not in cell bodies. Hence, it would appear that *hα*-syn was not overexpressed in hippocampal neurons but rather, that it spreads from neurons located in other anatomically connected areas where the AAV-*hα*-syn is overexpressed, such as the VTA. Although it is known that dopaminergic cells are the most abundant in the VTA (~65%), the predominant innervation reaching the hippocampus from the VTA is glutamatergic (~66–85%).<sup>18,60</sup> Accordingly, our results suggest that the hippocampal dysfunction in this model is due to a combination of impaired interaction between dopaminergic and glutamatergic projections from the VTA to the hippocampus.

Concomitant with the onset of *hα*-syn expression in the hippocampus (1 week p.i.), alterations to the expression of structural and functional proteins were demonstrated by proteomics and FASS-LTP, suggesting that glutamatergic and dopaminergic synaptic function is impaired by the accumulation of *hα*-syn. Studies with *α*-syn transgenic mice that have a widespread *hα*-syn pathology showed alterations to the presynaptic and postsynaptic compartments, and impaired hippocampal LTP, accompanied by well established learning and memory deficits.<sup>45,62–65</sup> However, in most of these studies dopaminergic degeneration is not detected or the nigrostriatal and mesolimbic dopaminergic systems are not fully characterized, key features of parkinsonism models. This study is the first to describe synaptic alterations at the earliest time points of *hα*-syn expression and at the beginning of cognitive decline in an animal model with known dopaminergic loss. We used a translational method to study LTP on isolated synaptosomes, identifying a subset of synaptosomes surface-labelled for both the postsynaptic GluA1 AMPAR subunit and presynaptic Nrx1β.<sup>51,54,55,66</sup> The changes in excitatory postsynaptic potentials evident through electrophysiological recording of LTP depend directly on changes in the density of postsynaptic AMPARs.<sup>22,23</sup> This approach is suited to screen multiple drugs in parallel and it can even be used with human brain samples from which viable synaptosomes can be efficiently obtained.<sup>55,67</sup> In our AAV-*hα*-syn animals, we observed impaired hippocampal cLTP from 1 week p.i., due to the enhanced basal GluA1 AMPAR expression in the postsynaptic membrane. It is well known that glutamatergic transmission is crucial for synaptic plasticity<sup>22</sup> and that it is modulated by dopamine.<sup>24</sup> Indeed, transgenic *hα*-syn mice exhibit basal hyperexcitability in the hippocampus,<sup>68</sup> and *in vitro* experiments show that *α*-syn inhibits LTP by enhancing basal synaptic transmission through the overactivation of NMDARs, which leads to a shift in AMPAR subunit composition.<sup>69</sup>

We studied the effect of PPX and L-DOPA on cLTP and both treatments, but especially L-DOPA at 4 weeks p.i., restored hippocampal cLTP in AAV-*hα*-syn animals by reversing the increase in the basal levels of postsynaptic AMPARs. Dopamine receptors interact directly with NMDARs<sup>59,60</sup> and AMPARs,<sup>61</sup> and while D1-like receptor agonists increase the phosphorylation of GluA1, those agonists of D2-like receptors dampen this modification,<sup>62,63</sup> an event that is essential to increase AMPAR conductance and that targets these receptors to the PSD.<sup>64,65</sup> In keeping with these effects, the AMPAR levels recovered better following incubation with L-DOPA than PPX. PPX is a D2-like receptor agonist with higher selectivity for D3Rs,<sup>70</sup> while L-DOPA, once converted into dopamine, activates both D1- and D2-like receptors.<sup>71</sup> Therefore, the differential activation of dopamine receptors may explain the stronger effect of L-DOPA over PPX in rescuing cLTP in AAV-*hα*-syn animals at 4

weeks p.i. Moreover, L-DOPA was previously shown to rescue hippocampal LTP,<sup>45,72,73</sup> whereas PPX does not rescue LTP in the DG<sup>73</sup> of parkinsonism models. L-DOPA only rescued cLTP at 4 weeks p.i., whereas PPX rescued cLTP at both 1 and 4 weeks p.i. This may be due to the direct stimulation of the corresponding receptors by dopaminergic agonists, while L-DOPA needs to be metabolized to dopamine in the presynaptic compartment before it can be released and activate its receptors.<sup>71</sup> Our proteomics results suggest a functional alteration of the presynaptic compartment at 1 week p.i., particularly in terms of intracellular trafficking and SV dynamics, which could impair the metabolism of L-DOPA and the release of dopamine from the presynapse. At 4 weeks p.i., only one deregulated protein was involved in synapse function, so the presynaptic alterations seem to be milder than at 1 week p.i., allowing the metabolism of L-DOPA, dopamine release and the rescue of LTP.

Interestingly, PPX had a negative effect on AAV-EVV animals compared to the vehicle, which is consistent with the inhibition of hippocampal LTP by PPX in healthy animals seen previously.<sup>34</sup> This effect could be due to the direct non-physiological overstimulation of D2R-like receptors, specially D3Rs, which have an affinity for dopamine more than 100-fold higher than that of D1Rs and D2Rs<sup>74</sup> and they are abundant in the limbic system.<sup>75</sup> This phenomenon could partially explain why L-DOPA has a positive effect on cognition in most Parkinson's disease patients whereas PPX is often associated with cognitive impairment.<sup>76,77</sup>

Accompanying the functional alterations, we identified changes in the expression of several proteins involved in synaptic organization and function soon after  $\alpha$ -syn overexpression (1 and 2 weeks p.i.). To our knowledge, this is the first time the hippocampal proteome has been analysed in parkinsonian animal models, especially at such early stages. Altered expression of synaptic proteins was recently described in the hippocampus of Parkinson's disease patients at advanced stages,<sup>44</sup> yet no studies have been carried out at the early stages of this disease. In the clustering analysis, only a few DEPs overlapped between the different time points studied. It must be considered that many of the DEPs participate in common biological processes and that most  $\alpha$ -syn interactors were identified at 1 week p.i. Hence, the presence of  $\alpha$ -syn in hippocampal synapses would initially appear to alter the expression of proteins that directly interact with  $\alpha$ -syn and, subsequently affect other proteins involved in related biological mechanisms. Thus,  $\alpha$ -syn triggers a chain reaction of pathological events in some biological pathways that influence synapses in which several proteins are involved, some in a more overarching manner, and others as part of a cascade of dynamic events exerting a stronger effect at a certain point. Many of the DEPs identified here participate in microtubule and actin cytoskeleton assembly and cytoplasmic transport. Intracellular transport of cargo, such as SVs at the presynapse and neurotransmitter receptors at the postsynapse, are key processes for correct neurotransmitter exocytosis and the induction of a postsynaptic response, respectively.<sup>78,79</sup> Cytoplasmic trafficking is regulated by Rab GTPases like RAB6B (upregulated at 1 week p.i.),<sup>80</sup> and motor proteins like the myosins MYH14 and MYO5A (downregulated at 2 weeks p.i.),<sup>81,82</sup> or kinesins like KLC2 (upregulated at 1 week p.i.).<sup>83</sup> These proteins, together with other DEPs like INPP4A or ANXA7, participate in the delivery of AMPAR and NMDAR to the PSD.<sup>84,85</sup> Moreover, PRRT2 and SNAP29 (downregulated at 2 weeks p.i.) modulate SV exocytosis<sup>86</sup> and turnover,<sup>87</sup> respectively. Another major regulator of intracellular vesicle trafficking is the ARF protein signalling pathway. IQSEC2 (downregulated at 2 weeks p.i.) is an activator of ARF6, and it is involved in surface AMPAR removal and the maintenance of long-term depression.<sup>88</sup> Other

crucial biological pathways are also deregulated at the earliest time points. The mitochondrial ATP synthase subunit ATP5MF is downregulated at 1 week p.i., suggesting a disruption of energy metabolism at the synapse.<sup>89</sup> Protein degradation through the lysosomal system may also be affected and VPS52, which participates in protein sorting to lysosomes through the Golgi-associated retrograde protein complex,<sup>90</sup> is downregulated at 2 weeks p.i. Interestingly, loss-of-function mutations in VPS35, another member of that family, are associated with inherited autosomal dominant Parkinson's disease cases.<sup>91</sup> Thus, the presence of  $\alpha$ -syn in hippocampal synapses interrupts the SV cycle at different steps, it hinders neurotransmitter receptor delivery and retrieval, and it interferes with normal mitochondrial function and protein degradation, contributing to synaptic dysfunction.

In contrast to the early alterations, prolonged  $\alpha$ -syn accumulation in the hippocampus is associated with a deregulation of neuronal homeostatic processes, such as the regulation of the membrane potential and of intracellular  $\text{Ca}^{2+}$  levels at 16 weeks p.i.  $\text{Ca}^{2+}$  acts as a second messenger in many signalling pathways that regulate morphology, synapse formation, excitability, neurotransmitter release and synaptic plasticity.<sup>92–94</sup> Calmodulin (CALM3) is downregulated at 16 weeks p.i., and it is a  $\text{Ca}^{2+}$ -adaptor protein that regulates several  $\text{Ca}^{2+}$  channels, including NMDARs,<sup>95</sup> and enzymes involved in synaptic plasticity such as CaMKII, calcineurin and PKA,<sup>96</sup> the latter also being downregulated at 16 weeks p.i. A decrease in CALM3 expression suggests that prolonged accumulation of  $\alpha$ -syn within the synapse may lead to overall and persistent synaptic dysfunction. Moreover, receptor-activated molecular signalling pathways are also deregulated at 16 weeks p.i. Notably, two glutamate receptors are downregulated at this time point, the GRIK2 kainate receptor and the GRM3 group II metabotropic receptor. Recently, activation of group II metabotropic receptors was shown to enhance the therapeutic benefits of L-DOPA and alleviate the psychosis-like behaviour in 6-OHDA rats and MPTP marmosets, suggesting these receptors to be potential targets for Parkinson's disease treatment.<sup>97</sup>

Some of the proteins identified here have been seen to be deregulated in the hippocampus of patients with advanced Parkinson's disease, including KRT1, KRT10, MAP2K1, PSD3, ARHGAP1, PRKACB, CSR1 and DDX39B.<sup>44</sup> Notably, one of the most severely downregulated proteins at 1 week p.i. is the amyloid precursor protein (APP), coinciding with the upregulation of other microtubule-associated proteins like MAP2, MAP2K1 and STMN1. In demented Parkinson's disease patients, co-morbid  $\alpha$ -syn, amyloid- $\beta$  and tau pathologies are frequently evident in the hippocampus,<sup>98</sup> suggesting that hippocampal synapses may be especially vulnerable to proteostatic alterations of APP and microtubule-associated proteins. Significantly, such protein alterations are not found in the striatum in this animal model<sup>39</sup> and thus, their deregulation might contribute specifically to cognitive decline. Moreover, one of the most strongly downregulated proteins at 2 weeks p.i. is LRP1, a member of the lipoprotein receptor family that acts as a cargo receptor at the synaptic membrane and that drives the ensuing endocytosis of its ligands including APP and TAU<sup>99,100</sup> and probably  $\alpha$ -syn.<sup>101</sup> This protein is diminished in the hippocampus of patients with amnesic mild cognitive impairment<sup>102</sup> and Alzheimer's disease,<sup>103</sup> as well as in the substantia nigra of patients with Parkinson's disease.<sup>104</sup>

Some limitations of this study must be acknowledged. Our functional and proteomic studies were performed on isolated hippocampal synaptosomes with neurotransmitter heterogeneity. The methods used to isolate specific populations of synaptosomes require staining for surface markers of synapses and additional processing time,<sup>105,106</sup> which would affect the viability of the

synaptosomes and the functional assessment of cLTP. Moreover, the immunofluorescent co-localization study was purely qualitative because we aimed to elucidate the nature of the VTA neurons and the axon terminals in the hippocampus that contain  $\alpha$ -syn, rather than quantifying the expression of these markers. Finally, the behavioural assessment revealed a tendency towards memory decline that was not statistically significant. However, many patients at the early stages of the disease experience subtle cognitive changes that are difficult to detect through global cognitive tests but that may be detected with specific memory tests. In some cases, while the values obtained do not reach statistical significance according to diagnostic criteria,<sup>107</sup> they are abnormal and noted clinically.<sup>108</sup> Our model recapitulates these mild deficits encountered in a relevant proportion of patients at the onset of motor manifestations.

Overall, our results suggest that  $\alpha$ -syn provokes early pathological changes to dopaminergic, glutamatergic and GABAergic axon terminals in the hippocampus, which contribute to the abnormal synaptic plasticity and cognitive deficits, and that can be modulated by L-DOPA but not PPX. These pathological changes in the hippocampus are probably due to early alterations to key proteins involved in cytoskeletal assembly, intracellular transport and SV dynamics crucial for neurotransmission. As such, our data pave the way for the future development of synapse-targeted therapies to enhance synaptic activity, specifically in the hippocampus, and ultimately to improve and/or maintain cognitive performance in Parkinson's disease patients.

## Data availability

An extended version of the 'Materials and methods' section is available in the [Supplementary material](#). The SWATH-MS data and search results files were deposited at the Proteome Xchange Consortium via the JPOST partner repository (<https://repository.jpostdb.org>),<sup>52</sup> under the identifiers PXD038793 for ProteomeXchange and JPST001951 for JPOST. Additional data that support the findings of this study are available from the corresponding author upon reasonable request.

## Acknowledgements

The authors would like to thank the CIMA-Universidad Navarra, IIS Biodonostia, Navarrabiomed, and the University of California Irvine for the use of their infrastructures and support.

## Funding

This study was funded by the Instituto de Salud Carlos III (ISCIII) through the project PI19/01915 Co-funded by the European Regional Development fund "A way to make Europe". A.B.-I. held a Predoctoral Research Fellowship from the Government of the Basque Country. L.M.-G. held a Predoctoral Research Fellowship from the Euskal Herriko Unibertsitatea (UPV/EHU). T.R.-C. and A.Q.-V. were funded by Centro de Investigación Biomédica en Red sobre Enfermedades Neurodegenerativas (CIBERNED). T.R.-C. held a Jesús de Gangoiti Barrera Foundation grant (Bilbao, Spain). G.A.P. is supported by the Alzheimer's Association (grant AARF-21-722869).

## Competing interests

M.C.R.-O. received financial support to attend scientific meetings and to deliver lectures from Boston Scientific, Abbvie and Insightec.

## Supplementary material

[Supplementary material](#) is available at *Brain* online.

## References

1. Poewe W, Seppi K, Tanner CM, et al. Parkinson Disease. *Nat Rev Dis Primers*. 2017;3:17013.
2. Postuma RB, Aarsland D, Barone P, et al. Identifying prodromal Parkinson's disease: Pre-motor disorders in Parkinson's disease. *Mov Disord*. 2012;27:617-626.
3. Schapira AHV, Chaudhuri KR, Jenner P. Non-motor features of Parkinson disease. *Nat Rev Neurosci*. 2017;18:435-450.
4. Kehagia AA, Barker RA, Robbins TW. Neuropsychological and clinical heterogeneity of cognitive impairment and dementia in patients with Parkinson's disease. *Lancet Neurol*. 2010;9:1200-1213.
5. Aarsland D, Batzu L, Halliday GM, et al. Parkinson disease-associated cognitive impairment. *Nat Rev Dis Primers*. 2021;7:47.
6. Smith C, Malek N, Grosset K, Cullen B, Gentleman S, Grosset DG. Neuropathology of dementia in patients with Parkinson's disease: A systematic review of autopsy studies. *J Neurol Neurosurg Psychiatry*. 2019;90:1234-1243.
7. Lisman J, Grace AA, Duzel E. A neoHebbian framework for episodic memory; role of dopamine-dependent late LTP. *Trends Neurosci*. 2011;34:536-547.
8. Fastenrath M, Coynel D, Spalek K, et al. Dynamic modulation of amygdala-hippocampal connectivity by emotional arousal. *J Neurosci*. 2014;34:13935-13947.
9. Rubin RD, Watson PD, Duff MC, Cohen NJ. The role of the hippocampus in flexible cognition and social behavior. *Front Hum Neurosci*. 2014;8:742.
10. LeGates TA, Kivarta MD, Tooley JR, et al. Reward behaviour is regulated by the strength of hippocampus-nucleus accumbens synapses. *Nature*. 2018;564:258-262.
11. González-Redondo R, García-García D, Clavero P, et al. Grey matter hypometabolism and atrophy in Parkinson's disease with cognitive impairment: A two-step process. *Brain*. 2014;137(Pt 8):2356-2367.
12. Martín-Bastida A, Delgado-Alvarado M, Navalpotro-Gómez I, Rodríguez-Oroz MC. Imaging cognitive impairment and impulse control disorders in Parkinson's disease. *Front Neurol*. 2021;12:733570.
13. Calabresi P, Castrioto A, di Filippo M, Picconi B. New experimental and clinical links between the hippocampus and the dopaminergic system in Parkinson's disease. *Lancet Neurol*. 2013;12:811-821.
14. Jay TM. Dopamine: A potential substrate for synaptic plasticity and memory mechanisms. *Prog Neurobiol*. 2003;69:375-390.
15. McNamara CG, Tejero-Cantero Á, Trouche S, Campo-Urriza N, Dupret D. Dopaminergic neurons promote hippocampal reactivation and spatial memory persistence. *Nat Neurosci*. 2014;17:1658-1660.
16. Alberico SL, Cassell MD, Narayanan NS. The vulnerable ventral tegmental area in Parkinson's disease. *Basal Ganglia*. 2015;5:51-55.
17. Giguère N, Burke Nanni S, Trudeau LE. On cell loss and selective vulnerability of neuronal populations in Parkinson's disease. *Front Neurol*. 2018;9:455.
18. Adeniyi PA, Shrestha A, Ogundele OM. Distribution of VTA glutamate and dopamine terminals, and their significance in CA1 neural network activity. *Neuroscience*. 2020;446:171-198.
19. Morales M, Margolis EB. Ventral tegmental area: Cellular heterogeneity, connectivity and behaviour. *Nat Rev Neurosci*. 2017;18:73-85.

20. Gcwensa NZ, Russell DL, Cowell RM, Volpicelli-Daley LA. Molecular mechanisms underlying synaptic and axon degeneration in Parkinson's disease. *Front Cell Neurosci.* 2021;15:44.
21. Holtmaat A, Caroni P. Functional and structural underpinnings of neuronal assembly formation in learning. *Nat Neurosci.* 2016;19:1553-1562.
22. Citri A, Malenka RC. Synaptic plasticity: Multiple forms, functions, and mechanisms. *Neuropsychopharmacology.* 2008;33:18-41.
23. Ho VM, Lee JA, Martin KC. The cell biology of synaptic plasticity. *Science.* 2011;334:623-628.
24. Lisman JE, Grace AA. The hippocampal-VTA loop: Controlling the entry of information into long-term memory. *Neuron.* 2005;46:703-713.
25. Yao WD, Spealman RD, Zhang J. Dopaminergic signaling in dendritic spines. *Biochem Pharmacol.* 2008;75:2055-2069.
26. Lee FJS, Xue S, Pei L, et al. Dual regulation of NMDA receptor functions by direct protein-protein interactions with the dopamine D1 receptor. *Cell.* 2002;111:219-230.
27. Ladepeche L, Yang L, Bouchet D, Groc L. Regulation of dopamine D1 receptor dynamics within the postsynaptic density of hippocampal glutamate synapses. *PLoS One.* 2013;8:e74512.
28. Liu XY, Chu XP, Mao LM, et al. Modulation of D2R-NR2B interactions in response to cocaine. *Neuron.* 2006;52:897-909.
29. Smith WB, Starck SR, Roberts RW, Schuman EM. Dopaminergic stimulation of local protein synthesis enhances surface expression of GluR1 and synaptic transmission in hippocampal neurons. *Neuron.* 2005;45:765-779.
30. Frey U, Schroeder H, Matthies H. Dopaminergic antagonists prevent long-term maintenance of posttetanic LTP in the CA1 region of rat hippocampal slices. *Brain Res.* 1990;522:69-75.
31. Rocchetti J, Isingrini E, Dal Bo G, et al. Presynaptic D2 dopamine receptors control long-term depression expression and memory processes in the temporal hippocampus. *Biol Psychiatry.* 2015;77:513-525.
32. Castro-Hernández J, Adlard PA, Finkelstein DI. Pramipexole restores depressed transmission in the ventral hippocampus following MPTP-lesion. *Sci Rep.* 2017;7:44426.
33. Swant J, Wagner JJ. Dopamine transporter blockade increases LTP in the CA1 region of the rat hippocampus via activation of the D3 dopamine receptor. *Learn Mem.* 2006;13:161-167.
34. Schepisi C, Pignataro A, Doronzio SS, et al. Inhibition of hippocampal plasticity in rats performing contrafreeloading for water under repeated administrations of pramipexole. *Psychopharmacology (Berl).* 2016;233:727-737.
35. Guo F, Zhao J, Zhao D, et al. Dopamine D4 receptor activation restores CA1 LTP in hippocampal slices from aged mice. *Aging Cell.* 2017;16:1323-1333.
36. Navakkode S, Chew KCM, Tay SJN, Lin Q, Behnisch T, Soong TW. Bidirectional modulation of hippocampal synaptic plasticity by dopaminergic D4-receptors in the CA1 area of hippocampus. *Sci Rep.* 2017;7:15571.
37. Ghiglieri V, Calabrese V, Calabresi P. Alpha-Synuclein: From early synaptic dysfunction to neurodegeneration. *Front Neurol.* 2018;9:295.
38. Calo L, Wegrzynowicz M, Santivañez-Perez J, Spillantini M G. Synaptic failure and  $\alpha$ -synuclein. *Mov Disord.* 2016;31:169-177.
39. Merino-Galan L, Jimenez-Urbieta H, Zamarbide M, et al. Striatal synaptic bioenergetic and autophagic decline in premotor experimental parkinsonism. *Brain.* 2022;145:2092-2107.
40. Garcia-Reitböck P, Anichtchik O, Bellucci A, et al. SNARE Protein redistribution and synaptic failure in a transgenic mouse model of Parkinson's disease. *Brain.* 2010;133(Pt 7):2032-2044.
41. Tozzi A, de Iure A, Bagetta V, et al. Alpha-Synuclein produces early behavioral alterations via striatal cholinergic synaptic dysfunction by interacting with GluN2D N-methyl-D-aspartate receptor subunit. *Biol Psychiatry.* 2016;79:402-414.
42. Xicoy H, Brouwers JF, Wieringa B, Martens GJM. Explorative combined lipid and transcriptomic profiling of substantia nigra and Putamen in Parkinson's disease. *Cells.* 2020;9:1966.
43. Nemani VM, Lu W, Berge V, et al. Increased expression of alpha-synuclein reduces neurotransmitter release by inhibiting synaptic vesicle recluster after endocytosis. *Neuron.* 2010;65:66-79.
44. Villar-Conde S, Astillero-Lopez V, Gonzalez-Rodriguez M, et al. The human hippocampus in Parkinson's disease: An integrative stereological and proteomic study. *J Parkinsons Dis.* 2021;11:1345-1365.
45. Costa C, Sgobio C, Siliquini S, et al. Mechanisms underlying the impairment of hippocampal long-term potentiation and memory in experimental Parkinson's disease. *Brain.* 2012;135(Pt 6):1884-1899.
46. Bereczki E, Branca RM, Francis PT, et al. Synaptic markers of cognitive decline in neurodegenerative diseases: A proteomic approach. *Brain.* 2018;141:582-595.
47. Paxinos G, Watson C. *The rat brain in stereotaxic coordinates.* 4th ed. Academic Press; 1998.
48. Zhou Y, Zhou B, Pache L, et al. Metascape provides a biologist-oriented resource for the analysis of systems-level datasets. *Nat Commun.* 2019;10:1523.
49. Oughtred R, Stark C, Breitkreutz BJ, et al. The BioGRID interaction database: 2019 update. *Nucleic Acids Res.* 2019;47:D529-D541.
50. Koopmans F, van Nierop P, Andres-Alonso M, et al. SynGO: An evidence-based, expert-curated knowledge base for the synapse. *Neuron.* 2019;103:217-234.e4.
51. Prieto GA, Trieu BH, Dang CT, et al. Pharmacological rescue of long-term potentiation in Alzheimer diseased synapses. *J Neurosci.* 2017;37:1197-1212.
52. Okuda S, Watanabe Y, Moriya Y, et al. jPOSTrepo: An international standard data repository for proteomes. *Nucleic Acids Res.* 2017;45:D1107-D1111.
53. Rodríguez-Chinchilla T, Quiroga-Varela A, Molinet-Droncha F, et al. [(18)F]-DPA-714 PET as a specific in vivo marker of early microglial activation in a rat model of progressive dopaminergic degeneration. *Eur J Nucl Med Mol Imaging.* 2020;47:2602-2612.
54. Prieto GA, Snigdha S, Baglietto-Vargas D, et al. Synapse-specific IL-1 receptor subunit reconfiguration augments vulnerability to IL-1 $\beta$  in the aged hippocampus. *Proc Natl Acad Sci U S A.* 2015;112:E5078-E5087.
55. Ahmad F, Jing Y, Lladó A, Liu P. Chemical stimulation of rodent and human cortical synaptosomes: Implications in neurodegeneration. *Cells.* 2021;10:1174.
56. Hirsch E, Graybiel AM, Agid YA. Melanized dopaminergic neurons are differentially susceptible to degeneration in Parkinson's disease. *Nature.* 1988;334:345-348.
57. Blesa J, Juri C, García-Cabezas MÁ, et al. Inter-hemispheric asymmetry of nigrostriatal dopaminergic lesion: A possible compensatory mechanism in Parkinson's disease. *Front Syst Neurosci.* 2011;5:92.
58. Hainmueller T, Bartos M. Dentate gyrus circuits for encoding, retrieval and discrimination of episodic memories. *Nat Rev Neurosci.* 2020;21:153-168.
59. Edelmann E, Lessmann V. Dopaminergic innervation and modulation of hippocampal networks. *Cell Tissue Res.* 2018;373:711-727.

60. Han Y, Zhang Y, Kim H, et al. Excitatory VTA to DH projections provide a valence signal to memory circuits. *Nat Commun.* 2020; 11:1466.
61. Ntamati NR, Lüscher C. VTA Projection neurons releasing GABA and glutamate in the dentate gyrus. *eNeuro.* 2016;3: ENEURO.0137-16.2016.
62. Masliah E, Rockenstein E, Mante M, et al. Passive immunization reduces behavioral and neuropathological deficits in an alpha-synuclein transgenic model of Lewy body disease. *PLoS One.* 2011;6:e19338.
63. Lim Y, Kehm VM, Lee EB, et al.  $\alpha$ -Syn suppression reverses synaptic and memory defects in a mouse model of dementia with Lewy bodies. *J Neurosci.* 2011;31:10076-10087.
64. Teravskis PJ, Covelo A, Miller EC, et al. A53t mutant alpha-synuclein induces tau-dependent postsynaptic impairment independently of neurodegenerative changes. *J Neurosci.* 2018;38:9754-9767.
65. Singh B, Covelo A, Martell-Martínez H, et al. Tau is required for progressive synaptic and memory deficits in a transgenic mouse model of  $\alpha$ -synucleinopathy. *Acta Neuropathol.* 2019; 138:551-574.
66. Marcatti M, Fracassi A, Montalbano M, et al.  $A\beta$ /tau oligomer interplay at human synapses supports shifting therapeutic targets for Alzheimer's disease. *Cell Mol Life Sci.* 2022;79:222.
67. Prieto GA, Cotman CW. On the road towards the global analysis of human synapses. *Neural Regen Res.* 2017;12: 1586-1589.
68. Tweedy C, Kindred N, Curry J, et al. Hippocampal network hyperexcitability in young transgenic mice expressing human mutant alpha-synuclein. *Neurobiol Dis.* 2021;149:105226.
69. Diógenes MJ, Dias RB, Rombo DM, et al. Extracellular alpha-synuclein oligomers modulate synaptic transmission and impair LTP via NMDA-receptor activation. *J Neurosci.* 2012;32: 11750-11762.
70. Beaulieu JM, Gainetdinov RR. The physiology, signaling, and pharmacology of dopamine receptors. *Pharmacol Rev.* 2011;63: 182-217.
71. Aldred J, Nutt JG. *Levodopa.* Academic Press; 2010:132-137.
72. Jalali MS, Sarkaki A, Farbood Y, et al. Transplanted wharton's jelly mesenchymal stem cells improve memory and brain hippocampal electrophysiology in rat model of Parkinson's disease. *J Chem Neuroanat.* 2020;110:101865.
73. Bonito-Oliva A, Pignatelli M, Spigolon G, et al. Cognitive impairment and dentate gyrus synaptic dysfunction in experimental parkinsonism. *Biol Psychiatry.* 2014;75:701-710.
74. Yang P, Perlmutter JS, Benzinger TLS, Morris JC, Xu J. Dopamine D3 receptor: A neglected participant in Parkinson disease pathogenesis and treatment? *Ageing Res Rev.* 2020;57:100994.
75. Prieto GA. Abnormalities of dopamine D3 receptor signaling in the diseased brain. *J Cent Nerv Syst Dis.* 2017;9:1179573517726335.
76. Roy MA, Doiron M, Talon-Croteau J, Dupré N, Simard M. Effects of antiparkinson medication on cognition in Parkinson's disease: A systematic review. *Can J Neurol Sci.* 2018;45:375-404.
77. Brusa L, Bassi A, Stefani A, et al. Pramipexole in comparison to l-dopa: A neuropsychological study. *J Neural Transm.* 2003;110: 373-380.
78. Waites C, Qu X, Bartolini F. The synaptic life of microtubules. *Curr Opin Neurobiol.* 2021;69:113-123.
79. Cingolani LA, Goda Y. Actin in action: The interplay between the actin cytoskeleton and synaptic efficacy. *Nat Rev Neurosci.* 2008;9:344-356.
80. Nyitrai H, Wang SSH, Kaeser PS. ELKS1 Captures rab6-marked vesicular cargo in presynaptic nerve terminals. *Cell Rep.* 2020; 31:107712.
81. Bu Y, Wang N, Wang S, et al. Myosin IIb-dependent regulation of actin dynamics is required for N-methyl-D-aspartate receptor trafficking during synaptic plasticity. *J Biol Chem.* 2015;290: 25395-25410.
82. Rudolf R, Bittins CM, Gerdes HH. The role of myosin V in exocytosis and synaptic plasticity. *J Neurochem.* 2011;116:177-191.
83. Hirokawa N, Noda Y, Tanaka Y, Niwa S. Kinesin superfamily motor proteins and intracellular transport. *Nat Rev Mol Cell Biol.* 2009;10:682-696.
84. Sasaki J, Kofuji S, Itoh R, et al. The PtdIns(3,4)P2 phosphatase INPP4A is a suppressor of excitotoxic neuronal death. *Nature.* 2010;465:497-501.
85. Li H, Liu S, Sun X, et al. Critical role for annexin A7 in secondary brain injury mediated by its phosphorylation after experimental intracerebral hemorrhage in rats. *Neurobiol Dis.* 2018;110: 82-92.
86. Valente P, Castroflorio E, Rossi P, et al. PRRT2 Is a key component of the  $Ca^{2+}$ -dependent neurotransmitter release machinery. *Cell Rep.* 2016;15:117-131.
87. Pan PY, Cai Q, Lin L, Lu PH, Duan S, Sheng ZH. SNAP-29-mediated modulation of synaptic transmission in cultured hippocampal neurons. *J Biol Chem.* 2005;280: 25769-25779.
88. Brown JC, Petersen A, Zhong L, et al. Bidirectional regulation of synaptic transmission by BRAG1/IQSEC2 and its requirement in long-term depression. *Nat Commun.* 2016;7:11080.
89. Ludtmann MHR, Angelova PR, Horrocks MH, et al.  $\alpha$ -synuclein oligomers interact with ATP synthase and open the permeability transition pore in Parkinson's disease. *Nat Commun.* 2018;9:2293.
90. Homma Y, Fukuda M. Knockout analysis of rab6 effector proteins revealed the role of VPS52 in the secretory pathway. *Biochem Biophys Res Commun.* 2021;561:151-157.
91. Nguyen M, Wong YC, Ysselstein D, Severino A, Krainc D. Synaptic, mitochondrial, and lysosomal dysfunction in Parkinson's disease. *Trends Neurosci.* 2019;42:140-149.
92. Berridge MJ. Neuronal calcium signaling. *Neuron.* 1998;21: 13-26.
93. Südhof TC. Calcium control of neurotransmitter release. *Cold Spring Harb Perspect Biol.* 2012;4:a011353.
94. Mateos-Aparicio P, Rodríguez-Moreno A. Calcium dynamics and synaptic plasticity. *Adv Exp Med Biol.* 2020;1131:965-984.
95. Villalobo A, Ishida H, Vogel HJ, Berchtold MW. Calmodulin as a protein linker and a regulator of adaptor/scaffold proteins. *Biochim Biophys Acta Mol Cell Res.* 2018;1865:507-521.
96. Xia Z, Storm DR. The role of calmodulin as a signal integrator for synaptic plasticity. *Nat Rev Neurosci.* 2005;6:267-276.
97. Frouni I, Hamadjida A, Kwan C, et al. Activation of mGlu(2/3) receptors, a novel therapeutic approach to alleviate dyskinesia and psychosis in experimental parkinsonism. *Neuropharmacology.* 2019;158:107725.
98. Irwin DJ, Lee VMY, Trojanowski JQ. Parkinson's disease dementia: Convergence of  $\alpha$ -synuclein, tau and amyloid- $\beta$  pathologies. *Nat Rev Neurosci.* 2013;14:626-636.
99. Rauch JN, Luna G, Guzman E, et al. LRP1 is a master regulator of tau uptake and spread. *Nature.* 2020;580:381-385.
100. Herz J, Strickland DK. LRP: A multifunctional scavenger and signaling receptor. *J Clin Invest.* 2001;108:779-784.
101. Sui YT, Bullock KM, Erickson MA, Zhang J, Banks WA. Alpha synuclein is transported into and out of the brain by the blood-brain barrier. *Peptides (NY).* 2014;62:197-202.
102. Sultana R, Banks WA, Butterfield DA. Decreased levels of PSD95 and two associated proteins and increased levels of BCL2 and caspase 3 in hippocampus from subjects with amnesic mild cognitive impairment: Insights into their potential

- roles for loss of synapses and memory, accumulation of A $\beta$ , and neurodegeneration in a prodromal stage of Alzheimer's disease. *J Neurosci Res.* 2010;88:469-477.
103. Shinohara M, Fujioka S, Murray ME, et al. Regional distribution of synaptic markers and APP correlate with distinct clinicopathological features in sporadic and familial Alzheimer's disease. *Brain.* 2014;137:1533-1549.
104. Wilhelmus MM, Bol JG, Van Haastert ES, et al. Apolipoprotein E and LRP1 increase early in Parkinson's disease pathogenesis. *Am J Pathol.* 2011;179:2152-2156.
105. Chinta SJ, Kumar MJ, Hsu M, et al. Inducible alterations of glutathione levels in adult dopaminergic midbrain neurons result in nigrostriatal degeneration. *J Neurosci.* 2007;27:13997-14006.
106. Paget-Blanc V, Pfeffer ME, Pronot M, et al. A synaptomic analysis reveals dopamine hub synapses in the mouse striatum. *Nat Commun.* 2022;13:3102.
107. Litvan I, Goldman JG, Tröster AI, et al. Diagnostic criteria for mild cognitive impairment in Parkinson's disease: Movement disorder society task force guidelines. *Mov Disord.* 2012;27:349-356.
108. Rodriguez-Oroz MC, Jahanshahi M, Krack P, et al. Initial clinical manifestations of Parkinson's disease: Features and pathophysiological mechanisms. *Lancet Neurol.* 2009;8:1128-1139.